Relation between the ratio of elastic work to the total work of indentation and the ratio of hardness to Young's modulus for a perfect conical tip

J. Chen and S.J. Bull[a)]
School of Chemical Engineering and Advanced Materials, Newcastle University, Merz Court, Newcastle upon Tyne NE1 7RU, United Kingdom

(Received 19 June 2008; accepted 21 August 2008)

A linear relationship between the ratio of elastic work to the total indentation work and hardness to reduced modulus, i.e., $W_e/W_t = \lambda H/E_r$, has been derived analytically and numerically in a number of studies and has been widely accepted. However, the scaling relationship between W_e/W_t and H/E_r has recently been questioned, and it was found that λ is actually not a constant but is related to material properties. In this study, a new relationship between W_e/W_t and H/E_r has been derived, which shows excellent agreement with numerical simulation and experimental results. We also propose a method for obtaining the elastic modulus and hardness of a material without invoking the commonly used Oliver and Pharr method. Furthermore, it is demonstrated that this method is less sensitive to tip imperfections than the Oliver and Pharr approach is.

I. INTRODUCTION

Based on the analysis of indentation by a cone, a linear relationship between the ratio of elastic work to the total work of indentation and hardness to reduced modulus has been proposed:[1]

$$\frac{W_e}{W_t} = \lambda \frac{H}{E_r} \quad . \tag{1}$$

Here $\lambda = \pi \tan \theta$, where θ is the half-included angle of the indenter. Using numerical simulation, a similar expression was derived by Cheng et al.[2,3] For a conical indenter with an equivalent projected area to a Berkovich indenter at a given depth $\lambda = 5.74$ using this equation. By curve fitting to finite element simulations, the value of λ is given as 4.678 in Ref. 4 and 5.04 in Ref. 5. In combination with the unloading stiffness, Eq. (1) has also been used to derive hardness and elastic modulus, and it was argued that it does not require an independent knowledge of the contact depth.[6] Thus it has been suggested that the problem to accurately determine contact depth when sink-in or pileup occurs can be avoided.[6] Whether this is valid or not will be discussed later in this paper.

Numerical simulations and experimental observations[6–8] demonstrate that after plastic deformation is well-established, the load–displacement (P-δ) curve follows Kick's law:

$$P_m = C\delta_m^2 \quad . \tag{2}$$

The total work is then given by

$$W_t = \frac{1}{3} P_m \delta_m \quad . \tag{3}$$

For materials without significant time-dependent behavior during the indentation process, it is often observed that the unloading curve can be described by a power law of the form[9]

$$P_m = B(\delta_m - \delta_r)^m \quad . \tag{4}$$

It has been shown that the exponent m is related to the shape of the deformed surface.[10] In general, the unloading exponent differs from 2 and the parameter B is therefore dependent on δ_m.[11]

Integrating the unloading curve gives the elastic work

$$W_e = \frac{1}{m+1} P_m(\delta_m - \delta_r) \quad . \tag{5}$$

Thus,

$$\frac{W_e}{W_t} = \frac{3}{m+1} - \frac{3}{m+1} \frac{\delta_r}{\delta_m} \quad . \tag{6}$$

The loading stiffness at peak load is given by

$$S_l = 2\frac{P_m}{\delta_m} \quad , \tag{7}$$

and the unloading stiffness at maximum load is given by

$$S_u = m\frac{P_m}{(\delta_m - \delta_r)} \quad . \tag{8}$$

Based on Sneddon's analysis,[12] the unloading stiffness can be also expressed as[9]

[a)]Address all correspondence to this author.
e-mail: s.j.bull@ncl.ac.uk
DOI: 10.1557/JMR.2009.0086

$$S_u = \frac{2\beta E_r}{\sqrt{\pi}}\sqrt{A_c} \quad , \tag{9}$$

where β takes account into the lateral displacement within the indentation.[13]

Combining Eqs. (7) and (8) yields

$$\frac{S_l}{S_u} = \frac{2}{m}\left(\frac{\delta_m - \delta_r}{\delta_m}\right) \quad . \tag{10}$$

Combining Eqs. (7) and (9), we also obtain

$$\frac{S_l}{S_u} = \frac{\pi}{\beta}\,\frac{H}{E_r}\,\frac{\delta_c \tan\theta}{\delta_m} \quad . \tag{11}$$

Thus,

$$\frac{W_e}{W_t} = \frac{3m}{2(m+1)}\,\frac{\pi \tan\theta}{\beta}\,\frac{H}{E_r}\,\frac{\delta_c}{\delta_m} \quad . \tag{12}$$

From Eq. (12), it can be seen that the linear scaling relationship between W_e/W_t and H/E_r is only valid if the unloading exponent m and the ratio of the contact depth over the maximum depth are constants.

It was observed that Eq. (1) with λ = 5.3 provides a reasonable global agreement with finite element method (FEM) data for a Berkovich indenter for a wide range of materials, but it was also found that the value of λ strongly depends on the work hardening behavior, particularly for soft metals.[14] Unfortunately, the analysis given by Alkorta et al.[14] ends at this point, and no further explanation is given. Actually, the dependency of λ on the ratio of H/E_r had also been noticed by Choi et al.[15] By careful investigation of experimental results, they found different values of λ are required for soft metals and hard ceramics respectively (e.g., λ = 7.3, when $W_e/W_t < 0.15$; λ = 5.17, when $W_e/W_t \geq 0.15$). However, it is difficult to understand why there should be a sharp jump in the value of λ when W_e/W_t approaches 0.15. Therefore, a more comprehensive relationship between the ratio of elastic work over the total work of indentation and hardness over reduced modulus is required. This is the subject of this paper.

II. ANALYTICAL MODEL

Some basic questions need to be addressed before we try to further develop the relationship between W_e/W_t and H/E_r. It is essential to understand why Eq. (1) was proposed and the circumstances when it is invalid. This is discussed in this section before introducing a new model.

As shown by Eq. (12), Eq. (1) can be derived if the unloading exponent m and the ratio of the contact depth over the maximum depth are constants. The contact depth given by Sneddon[12] for an elastic contact problem is

$$\delta_c = \frac{2}{\pi}\delta_m \quad . \tag{13}$$

At the same time if we assume that m is a constant [e.g., $m = 2$, which is the extreme case when Y/E approaches 0 and there is no work hardening (i.e., the work hardening exponent $n = 0$)], we get

$$\frac{W_e}{W_t} = \frac{2\tan\theta}{\beta}\,\frac{H}{E_r} \quad . \tag{14}$$

A similar expression is obtained elsewhere.[14] For a conical indenter with a half-included angle of 70.3°, the coefficient multiplying H/E_r is about 5.25 (with β = 1.065[9]), which is close to the 5.3 suggested by Alkorta.[14] However, it is obvious that for elastic–plastic contact, Eq. (13) is not correct. Furthermore, sink-in and pileup will definitely influence the ratio of real contact depth over maximum depth. On the other hand, m does not equal 2 in general as mentioned previously. That is why a different scaling relationship between W_e/W_t and H/E_r is proposed.

From Eq. (6), it can be seen that the fundamental relationship between W_e/W_t and H/E_r is based on the relationship between H/E_r and δ_r/δ_m. A few expressions have been proposed to describe δ_r/δ_m in terms of H/E_r[2,3,16–19] as discussed in our previous study where a nonlinear expression was developed,[19] which is more generally applicable. The main points of the derivation are reproduced in the following.

The nanoindentation hardness is given by

$$H = P/A_c \quad , \tag{15}$$

where A_c is the contact area given by $\pi(\delta_c \tan\theta)^2$ for a perfect conical tip with half-angle θ.

Rearranging Eq. (8) gives, $\delta_m - \delta_r = mP_m/S$ and the elastic deflection of the surface during indentation is given by

$$\delta_m - \delta_c = \varepsilon\frac{P_m}{S_u} \quad . \tag{16}$$

If Eqs. (9), (15), and (16) are combined we get

$$\delta_m = \left[1 + \frac{\pi\varepsilon}{2\beta}\,\frac{H}{E_r}\tan(\theta)\right]\delta_c \quad . \tag{17}$$

If Eqs. (8), (9) and (17) are combined we obtain

$$\frac{\delta_r}{\delta_m} = 1 - \frac{m\pi}{2\beta}\,\frac{H}{E_r}\tan\theta\left(\frac{1}{1 + \frac{\pi}{2\beta}\varepsilon\frac{H}{E_r}\tan\theta}\right) \quad , \tag{18}$$

where the value of m can be obtained by fitting finite element simulations or experimental load–displacement results. The same expression can be derived in a different way as described in Ref. 19. Equation (18) indicates that the relationship between δ_r/δ_m and H/E_r is actually not linear and is dependent on m. It should be pointed

out that the actual contact depth may differ from that given in Eq. (16) in the presence of pileup and sink-in. However, Eq. (18) has been validated even for materials displaying a small amount of pileup and sink-in during indentation. Considering that the pileup is related to Y/E_r and the work hardening exponent n, this implies that m is also dependent on Y/E_r and n. This is not surprising because the parameter m is related to the shape of deformed surface, and Y/E_r and n determine the shape of the deformed surface when the Poisson's ratio ν and the half-included angle of the indenter θ are fixed.

Combining Eqs. (6) and (18) gives,

$$\frac{W_e}{W_t} = \frac{3m\pi}{2\beta(m+1)} \frac{H}{E_r} \tan\theta \left(\frac{1}{1+\frac{\pi\varepsilon}{2\beta}\frac{H}{E_r}\tan\theta} \right) \quad . \tag{19}$$

The same equation can be derived if we substitute Eq. (17) into Eq. (12). Equation (19) clearly shows that the relationship between W_e/W_t and H/E_r is actually nonlinear.

III. FINITE ELEMENT MODEL

Since a three-dimensional (3D) model produces results similar to those of a two-dimensional (2D) model when solving elastic-plastic problems,[20] the 2D rigid-flexible half model was adopted here for computing efficiency. The commercial finite element program ANSYS 9.0 (ANSYS, Inc., Canonsburg, PA) was used in this study. The effective half-included angle of the conical indenter used here is 70.3° (with equivalent projected area to a Berkovich tip).

The elastic properties for the diamond tip (E = 1141 GPa, ν = 0 .07) were fixed, and it is assumed to be elastically deformed for all models. A 2D 6-Node Triangle Structural Solid element was used to model the 2D diamond indenter. The mesh, boundary conditions applied, and the contact pairs are the same as those described in our previous study.[19] The interface between the indenter and the specimen is assumed frictionless. Contact depth and residual depth are directly measured from the deformation profile; thus we consider the effect of pileup and sink-in when calculating the hardness. To maximize the speed of simulations, displacement control is preferred, and a maximum penetration of 400 nm is adopted for all the materials investigated here.

Both elastic–perfectly plastic solid materials and materials with power-law work hardening behavior were examined in this study. In the simulations, the Young's modulus E and Poisson's ratio ν for the specimens were fixed at E = 70 GPa and ν = 0.25, respectively. The yield stress Y was varied from 0.07 to 7 GPa. For work hardening materials, the work hardening exponent was varied from 0 to 0.5. This leads to ratios of modulus over yield strength in the range of 10–1000, which covers most ceramics and metals. Time-dependent behavior such as creep is not included in the model; this may have a significant influence on the results, which makes the analysis more complex.[21] The basic stress–strain (σ-ε) relationship used in the model is

$$\sigma = \begin{cases} E\varepsilon, & \text{for } \varepsilon \le \dfrac{Y}{E} \\ K\varepsilon^n, & \text{for } \varepsilon \ge \dfrac{Y}{E} \end{cases} , \tag{20}$$

where K is a constant and n is the work hardening exponent.

IV. RESULTS AND DISCUSSION

A. Relationship between δ_r/δ_m and H/E_r

As discussed previously, the parameter m is related to Y/E_r and n; however, it is difficult to derive an analytical expression between them. From FEM studies carried out in this study, we have found an approximately linear relationship between m and the work hardening exponent n [Eq. (21)] when $0.001 < Y/E_r < 0.1$.

$$m = 1.24 + 0.2n \quad . \tag{21}$$

This generates values of m between 1.24 and 1.34 for elastic–perfectly plastic solids and work hardening materials as n is normally less than 0.5. It falls in the range determined by Pharr et al.[10] (i.e., m = 1.16 to 1.48). It should be noted that time-dependent behavior can significantly affect the unloading curve (and thus the value of m), and the analysis here is not valid for materials showing significant time-dependent behavior during the indentation tests.

Thus, Eq. (18) can be rewritten by replacing m with n:

$$\frac{\delta_r}{\delta_m} = 1 - \frac{\pi(1.24+0.2n)}{2\beta} \frac{H}{E_r} \tan\theta \left(\frac{1}{1+\frac{\pi\varepsilon}{2\beta}\frac{H}{E_r}\tan\theta} \right) \quad . \tag{22}$$

Comparisons were made between Eq. (22) developed in this study and other models, which are plotted in Figs. 1–3.

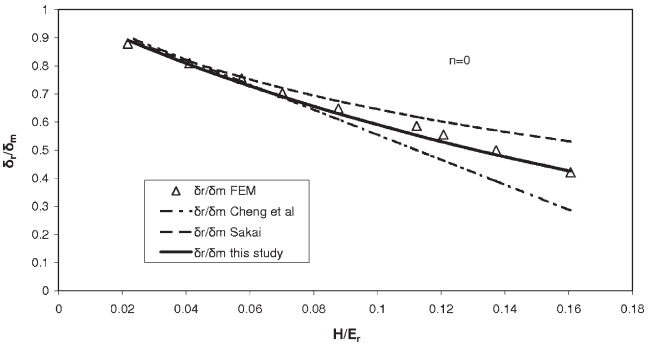

FIG. 1. Comparison of the relationship between the ratio of residual depth to maximum depth and the ratio of hardness to contact modulus for elastic–perfectly plastic materials (n = 0) determined by different workers and finite element simulation.

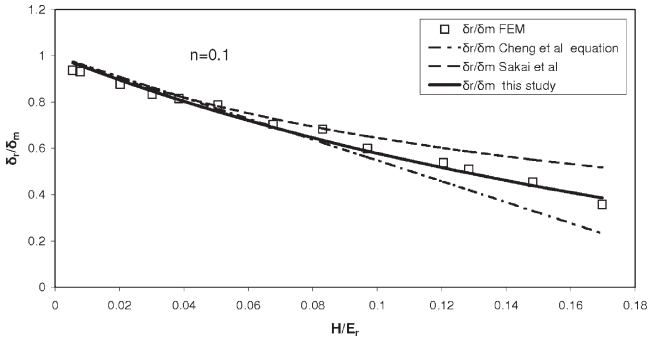

FIG. 2. Comparison of the relationship between the ratio of residual depth to maximum depth and the ratio of hardness to contact modulus for materials with work hardening (n = 0.1) determined by different workers and finite element simulation.

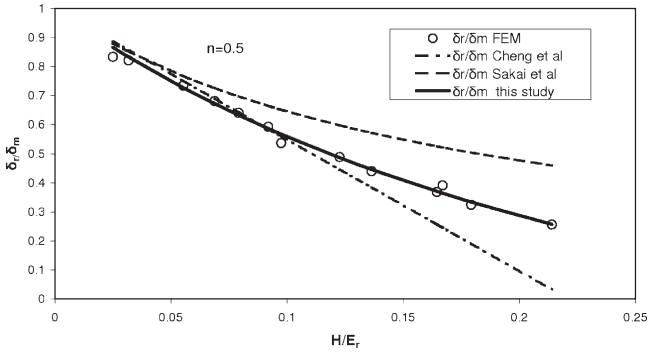

FIG. 3. Comparison of the relationship between the ratio of residual depth to maximum depth and the ratio of hardness to contact modulus for materials with severe work hardening (n = 0.5) determined by different workers and finite element simulation.

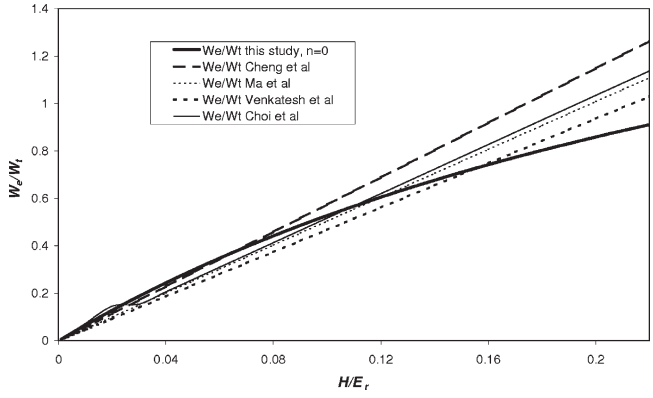

FIG. 4. Comparison of the expression to describe W_e/W_t in terms of H/E_r developed in this study and literature expressions for elastic–perfectly plastic materials.

The equation derived by Cheng et al.[2,3] gives a good fit only when H/E_r is less than 0.1. This is not surprising since they argued that their equation is valid for δ_r/δ_m more than 0.4, which requires H/E_r to be less than 0.1 for a perfect conical indenter with semi-angle of 70.3°. When $H/E_r > 0.1$, the equation developed in Refs. 2 and 3 significantly diverges from the finite element data for both elastic–perfectly plastic solids and work hardening materials. Other models, for example, the nonlinear equation developed by Sakai in Ref. 16 significantly diverge at an earlier stage ($H/E_r > 0.05$). In contrast, Eq. (22) developed in this study shows excellent agreement with the FE simulations.

B. Relationship between W_e/W_t and H/E_r

Substituting Eq. (21) into Eq. (19) gives

$$\frac{W_e}{W_t} = \frac{1.5(1.24+0.2n)\pi}{(0.24+0.2n)\beta}\,\frac{H}{E_r}\tan\theta\left(\frac{1}{1+\frac{\pi\varepsilon}{2\beta}\frac{H}{E_r}\tan\theta}\right) \quad . \tag{23}$$

An alternative nonlinear relationship between W_e/W_t and H/E_r was derived elsewhere by Malzbender et al.[18]

$$\frac{W_e}{W_t} = \left(\frac{\varepsilon}{2}+\frac{\beta}{\pi\frac{H}{E_r}\tan\theta}\right)^{-1} \quad . \tag{24}$$

To justify which models are better, experimental validation is required. For example, taking 1070 steel, the values of the reduced modulus (indented by a diamond Berkovich tip) and hardness are 182 and 9.5 GPa, respectively, and the measured value of W_e/W_t is 0.298.[22] The model proposed in Ref. 4 gives a value of 0.227 for W_e/W_t (with a deviation of 25%), the expression developed in Refs. 2 and 3 gives a value of 0.287 for W_e/W_t (with a deviation of 5%), and the approach of Alkorta et al.[14] gives a value of 0.277 for W_e/W_t (with a deviation of 7%). Other approaches give a value of 0.270,[15] 0.263,[5] and 0.245[23] for W_e/W_t. However, the equation proposed in this study gives a value of 0.296, which agrees almost perfectly with the experimentally measured value (the difference is less than 1%). Similar good agreement is produced for a range of materials with different H/E_r (Figs. 4–8).

Figure 6 depicts a comparison of the different expressions proposed to describe W_e/W_t in terms of H/E_r and finite element simulation taken from the literature. Only some of the linear expressions were plotted to for comparison as the relationship between W_e/W_t and H/E_r is actually nonlinear.[14] Equation (23) developed in this study gives the best agreement with FEM data. Figure 4 also shows that all the expressions proposed in the literature lead to a unity value for W_e/W_t when $H/E_r < 0.2$. However, experimental data show that even when H/E_r is around 0.25, the value of W_e/W_t is less than 1.[24] This agrees well with our prediction (see Figs. 5 and 6).

For clarification, a separate comparison between the variation of W_e/W_t with H/E_r determined in this study [i.e., Eq. (23)] and the linear and nonlinear expressions given by Malzbender et al.[6,18] [i.e., Eqs. (14) and (24)] is depicted in Fig. 9. Again, the linear plot deviates

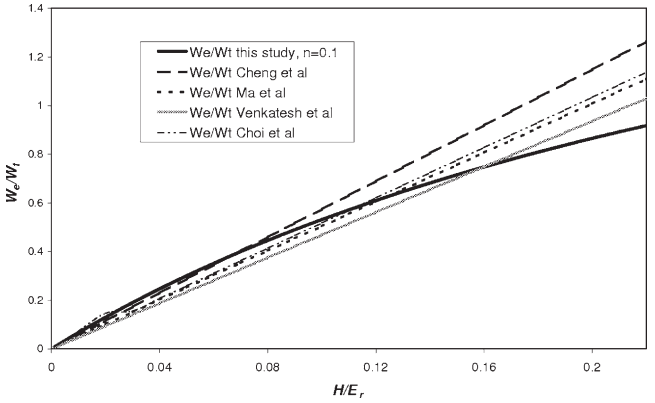

FIG. 5. Comparison of the expression to describe W_e/W_t in terms of H/E_r developed in this study and literature expressions for materials with a work hardening exponent of 0.1.

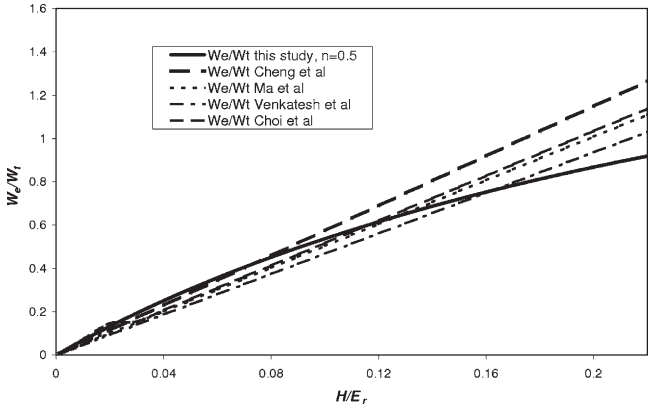

FIG. 6. Comparison of the expression to describe W_e/W_t in terms of H/E_r developed in this study and literature expressions for materials with a work hardening exponent of 0.5.

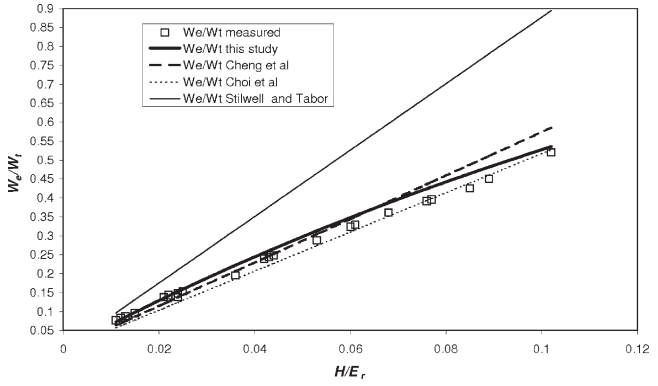

FIG. 7. Comparison of the expression to describe W_e/W_t in terms of H/E_r developed in this study and literature expressions as well as measured data from Stilwell and Tabor.[1]

significantly from that developed in this study. The nonlinear relationship proposed by Malzbender et al.[18] shows a similar trend in the W_e/W_t versus H/E_r plot, but it significantly overestimates the value of W_e/W_t for soft materials. Again, it leads to $W_e/W_t \approx 1$ when H/E_r approaches 0.2, which is not correct as mentioned above.

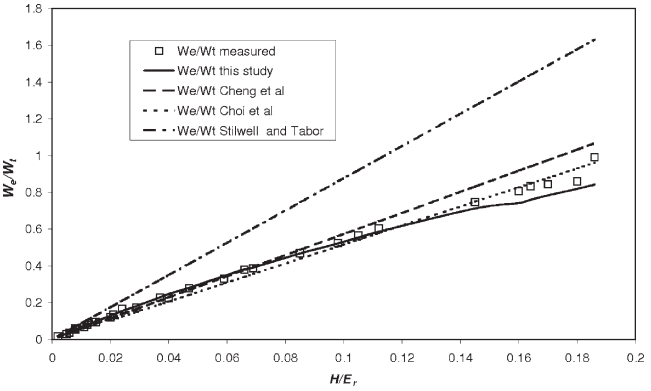

FIG. 8. Comparison of the expression to describe W_e/W_t in terms of H/E_r developed in this study and literature expressions as well as measured data from Alkorta.[14]

From Fig. 9, it can be seen that the curves for W_e/W_t versus H/E_r are almost indistinguishable for all levels of work hardening. It might be argued that the work hardening should have a big effect on very soft metals, and this may just be hidden in a global plot over a wide range of H/E_r. Therefore, a localized plot for soft materials with various work hardening exponents is plotted in Fig. 10. It can be clearly seen that for the model presented in this study the effect of work hardening on W_e/W_t is negligible even for very soft metals.

C. Alternative method for obtaining *H* and E_r

Combining Eqs. (9) and (15), we obtain

$$\frac{H}{E_r^2} = \frac{4\beta^2 P}{\pi S_u^2} \quad . \tag{25}$$

Rewriting Eqs. (18) and (19), we get

$$\frac{H}{E_r} = \frac{2\beta\cot\theta}{\pi} \frac{\left(1-\frac{\delta_r}{\delta_m}\right)}{(1.24+0.2n)-\left(1-\frac{\delta_r}{\delta_m}\right)\varepsilon} \quad , \tag{26}$$

and

$$\frac{H}{E_r} = \frac{\beta W_e/W_t}{\frac{1.5\pi(1.24+0.2n)}{(2.24+0.2n)} - \pi\varepsilon W_e/2W_t}\cot\theta \quad . \tag{27}$$

Combining Eqs. (25) and (26) we obtain

$$E_r = \frac{\left(1-\frac{\delta_r}{\delta_m}\right)S_u^2\cot\theta}{2\beta P_m\left[(1.24+0.2n)-\left(1-\frac{\delta_r}{\delta_m}\right)\varepsilon\right]} \quad , \tag{28a}$$

$$H = \frac{\left(1-\frac{\delta_r}{\delta_m}\right)^2 S_u^2\cot^2\theta}{\pi\beta P_m\left[(1.24+0.2n)-\left(1-\frac{\delta_r}{\delta_m}\right)\varepsilon\right]^2} \quad , \tag{28b}$$

while combining Eqs. (25) and (27) yields

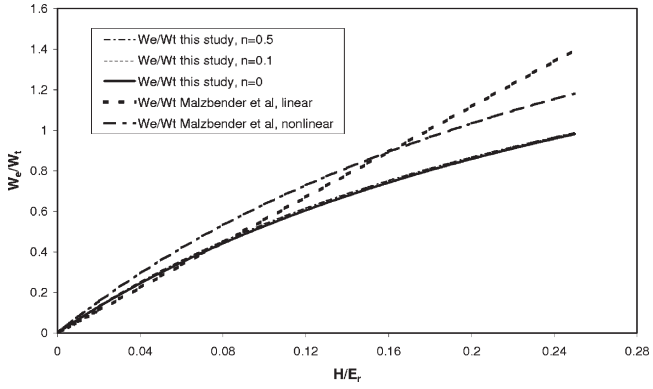

FIG. 9. Comparison of the variation of W_e/W_t with H/E_r determined in this study [i.e., Eq. (23)] and the linear and nonlinear expressions given by Malzbender et al.[6,18] [i.e., Eqs. (14) and (24)].

$$E_r = \frac{W_e/W_t}{\frac{1.5\pi(1.24+0.2n)}{(2.24+0.2n)} - \pi\varepsilon W_e/2W_t}\cot\theta \Big/ \frac{4\beta\, P_m}{\pi S_u^2} \quad , \quad (29a)$$

$$H = \left(\frac{W_e/W_t}{\frac{1.5\pi(1.24+0.2n)}{(2.24+0.2n)} - \pi\varepsilon W_e/2W_t}\right)^2 \Big/ \frac{4P_m}{\pi S_u^2} \quad . \quad (29b)$$

These provide alternative approaches to obtain the values of hardness and reduced modulus without independent measurement of the contact depth. Of the two the energy based approach is more promising since the accurate measurement of residual depth is not easy, and this can cause significant error in the ratio of residual depth over maximum depth, but measurement errors have only a negligible influence on W_e/W_t.

It has been previously argued that an energy-based approach could be used to derive hardness and elastic modulus and avoid problems caused by pileup and sink-in.[6,18] However, in cases where significant pileup (i.e., the real contact depth exceeds the maximum penetration depth) occurs around the indentation, separate microscopy assessment of the indentation profile is still required to obtain an accurate value of hardness and elastic modulus. The reason is that in this analysis, it is assumed the contact depth is the difference between the total displacement and the elastic displacement of the surface at the edge of the impression, which does not take account of any pileup. We also need to bear in mind that only part of the pileup is actually in contact with indenter. Therefore, if the actual contact edge is not significantly above the surface (i.e., the amount of pile-up is small), the models presented here work reasonably well because the effect of pileup and sink-in can be included in the parameter m for the material properties given in this study as discussed in Sec. II. On the other hand, with the energy-based approach [e.g., Eq. (29)], the tip area function calibration is not necessary anymore, which saves time, and it avoids possible errors from fitting a nonphysical area function to the measured data.

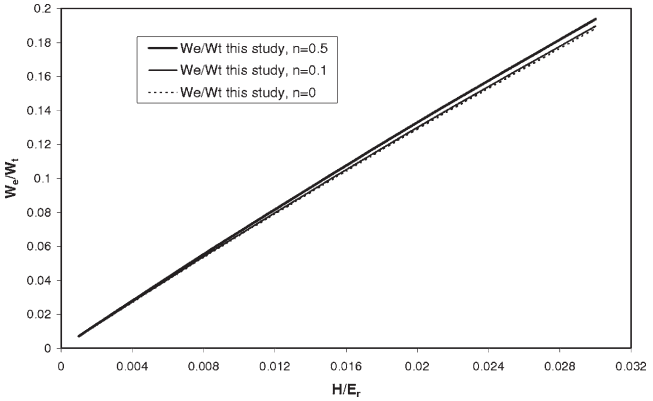

FIG. 10. Localized plot of W_e/W_t versus H/E_r for soft materials (with low H/E_r) with different levels of work hardening. The effect of work hardening is negligible.

To illustrate the utility of this approach, Fig. 11 displays a comparison of the determination of hardness and reduced modulus based on the Oliver and Pharr method (O & P) and the model suggested here [i.e., Eq. (29)] for fused silica, which is a material that is not well handled by previous energy-based hardness models due to its high H/E. The values of reduced modulus determined by both methods at various loads agree very well. For the hardness, reasonably good agreement is achieved at large penetrations where tip blunting has a negligible effect on the contact area. However, at low penetrations where tip blunting is critical, a significant discrepancy between these two approaches is observed. This could be due to the erroneous experimental fitting of the tip area function. On the other hand, it may suggest that the model requires modification for the truncated tip, and a length-scale parameter (i.e., tip radius) should be included in the model as suggested in Refs. 11, 25, and 26. However, the fact that the hardness determined by the new model is approximately constant over a large load range, whereas the hardness determined by the Oliver and Pharr method increases at low loads, implies that the tip calibration is in error. Tip defects have a considerable influence on data obtained by nanoindentation, and methods to accurately account for tip shape (both in terms of tip end radius[27] and the instantaneous effective tip angle[28]) or reduce its effect are essential. The reduction in hardness at the lowest loads is due to the transition from elastic to plastic behavior. There is also considerable scatter in E_r at low loads where W_e is of similar magnitude to W_t, and significant errors are expected in the model developed here due to limitations in determining these values with sufficient accuracy. In such cases, the value of m is also likely to change; in other words, m can be also related to the tip radius. More comparisons of hardness and reduced modulus values for other materials (such as aluminum and soda-lime glass as depicted in Figs. 12 and 13, respectively) obtained by the O & P

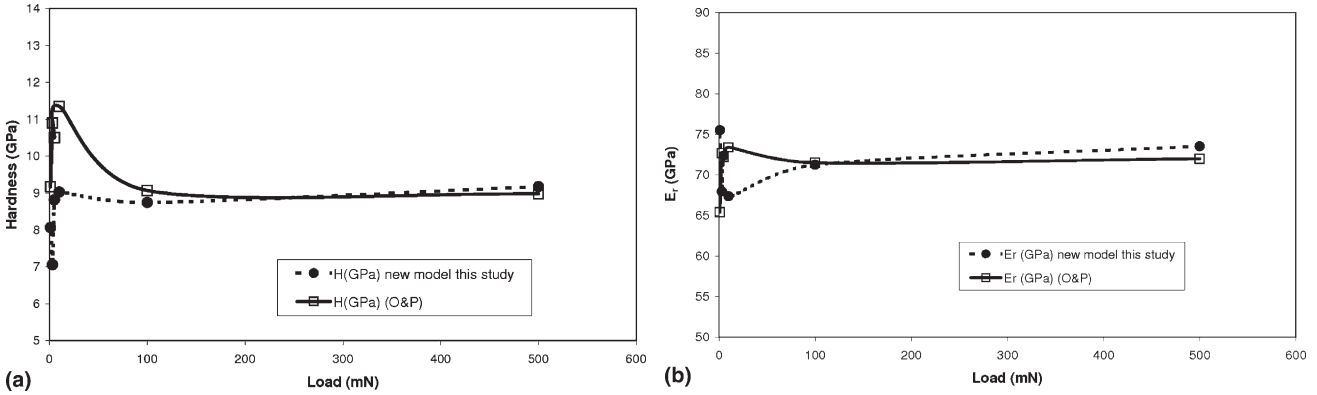

FIG. 11. Comparison of (a) hardness and (b) reduced modulus of fused silica using the Oliver and Pharr method (O & P) and the new model suggested here [i.e., Eq. (28)].

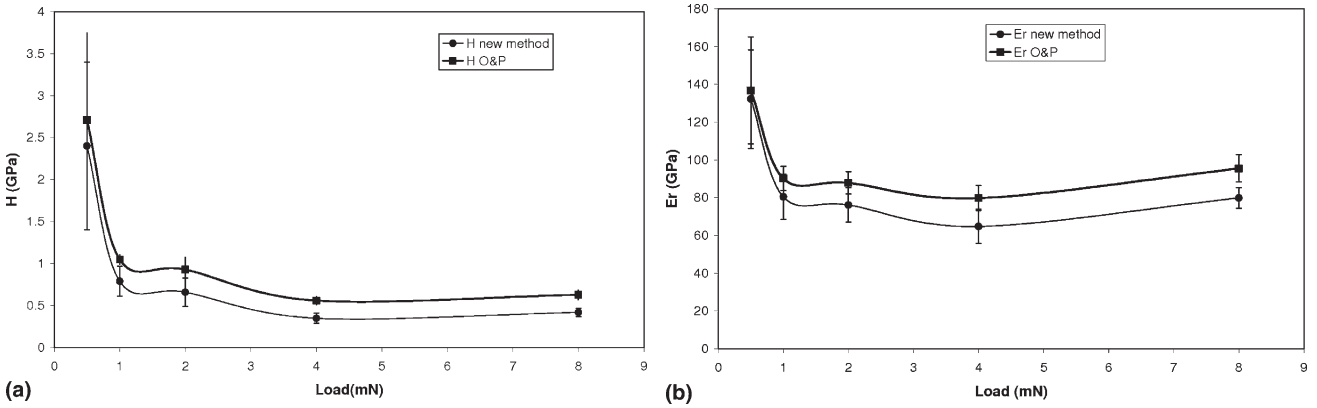

FIG. 12. Comparison of (a) hardness and (b) reduced modulus of aluminum using O & P and the new model suggested here [i.e., Eq. (28)].

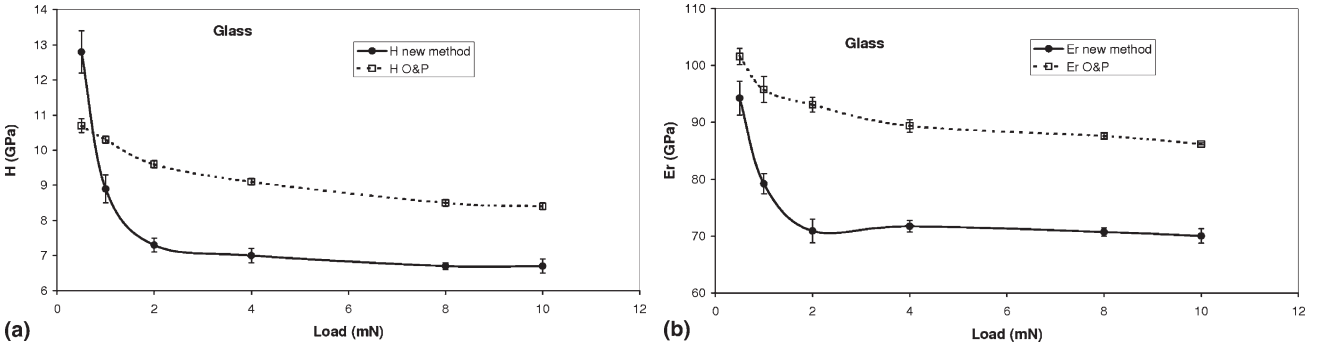

FIG. 13. Comparison of (a) hardness and (b) reduced modulus for soda lime glass using O & P and the new model suggested here [i.e., Eq. (28)].

method and the method presented here have been made, and it demonstrates that the method presented here gives more reasonable results when tested by a used indenter at low loads. From Figs. 12 and 13, it is obvious that significant discrepancy was observed. As the testing load was low (so was the penetration), the tip blunting tends to play an important role. Although the assumption of a spherical truncated tip is reasonable for a new tip, there is no reason for this to be true after many indentation tests. Thus, the analytical expression for describing the tip shape is not realistic. It is also very unlikely for experimentalists to update the area function calibrations every time before tests. There is also no guideline for how often the area function should be updated. Therefore, it can lead to overestimation of the measured hardness and elastic modulus if the area function is not updated in time. On the other hand, the initial tip area function is a

good approximation at given range of contact depth. In practice, the actual contact depth for some materials may be outside this range; therefore, we may not expect reasonable results in such cases. Further work is underway to validate the new approach on a larger range of materials with different Y/E.

Tests have also been performed on metallic materials including copper and gold. The hardness values obtained by the new method are closer to the results after pileup correction compared to the common Oliver and Pharr method. Another essential issue that must be emphasized is the influence of the proportion of the unloading curve, which is fitted to determine the unloading stiffness. This may also affect the derived elastic modulus. This is particularly crucial for materials that show time-dependent behavior, even if this is limited when indentation is performed at room temperature. The upper one third is the recommended fitting range for the unloading curve according to Oliver and Pharr. If we change this even slightly, even if enough data points are ensured, the derived values of elastic modulus may change, although there is no obvious change in the hardness. This problem can be circumvented using the equations developed here.

For soda-lime glass there is a much bigger difference between the Oliver and Pharr hardness and modulus values and those determined by the method developed here. Using Eq. (28), the values are lower but constant as a function of depth and closer to values measured by other techniques (microhardness and bending tests). More work is underway to understand the reasons for the discrepancy.

V. CONCLUSIONS

The existing linear relationships between δ_r/δ_m and H/E_r developed by means of analytical or numerical methods have been examined. It was found that they provide a good fit for materials with low H/E_r; however, when H/E_r is bigger than 0.1, significant deviation occurs. A nonlinear analytical expression between δ_r/δ_m and H/E_r is proposed, and this has been verified by finite element simulations for elastic–perfectly plastic materials and power law work hardening materials.

The finite element simulations demonstrate that the existing linear relationships between the elastic work over total work and hardness over the reduced modulus reported in the literature and commonly accepted is not correct. A new model has been developed for the relationship between W_e/W_t and H/E_r, which agrees well with the numerical simulation results and experimental data.

Based on the newly developed relationship between δ_r/δ_m and H/E_r in combination with existing numerical and analytical models, a new expression has been developed for the relationship between W_e/W_t and H/E_r.

The elastic modulus and hardness can be directly measured based on knowledge of the maximum load, unloading stiffness, and W_e/W_t (or δ_r/δ_m). This method is less sensitive to tip imperfection compared to the common Oliver and Pharr approach.

ACKNOWLEDGMENTS

This research was supported by The Engineering and Physical Sciences Research Council (EPSRC) through the multiscale modeling initiative. Prof. S. Roy, Dr. L. Siller, and Mr. P. Cox at Newcastle University are acknowledged for providing some samples for tests.

REFERENCES

1. N.A. Stilwell and D. Tabor: Elastic recovery of conical indentations. *Proc. Phys. Soc. London* **78,** 169 (1961).
2. Y-T. Cheng, Z. Li, and C-M. Cheng: Scaling relationships for indentation measurements. *Philos. Mag. A* **82,** 1821 (2002).
3. Y-T. Cheng and C-M. Cheng: Relationships between hardness, elastic modulus, and the work of indentation. *Appl. Phys. Lett.* **73,** 614 (1998).
4. A.E. Giannakopoulos and S. Suresh: Determination of elastoplastic properties by instrumented sharp indentation. *Scr. Mater.* **40,** 1191 (1999).
5. D. Ma, W. Chung, J. Liu, and J. He: Determination of Young's modulus by nanoindentation. *Sci. China, Ser. E* **47,** 398 (2004).
6. J. Malzbender: Comment on the determination of mechanical properties from the energy dissipated during indentation. *J. Mater. Res.* **20,** 1090 (2005).
7. W.C. Oliver: Alternative technique for analyzing instrumented indentation data. *J. Mater. Res.* **16,** 3202 (2001).
8. S.V. Hainsworth, H.W. Chandler, and T.F. Page: Analysis of nanoindentation load–displacement loading curves. *J. Mater. Res.* **11,** 1987 (1996).
9. W.C. Oliver and G.M. Pharr: An improved technique for determining hardness and elastic-modulus using load and displacement sensing indentation experiments. *J. Mater. Res.* **7,** 1564 (1992).
10. G.M. Pharr and A. Bolshakov: Understanding nanoindentation unloading curves. *J. Mater. Res.* **17,** 2660 (2002).
11. Y-T. Cheng and C-M. Cheng: Scaling, dimensional analysis, and indentation measurements. *Mater. Sci. Eng., R* **44,** 91 (2004).
12. I.N. Sneddon: The relation between load and penetration in the axisymmetric Boussinesq problem for a punch of arbitrary profile. *Int. J. Eng. Sci.* **3,** 47 (1965).
13. J.C. Hay, A. Bolshakov, and G.M. Pharr: A critical examination of the fundamental relations used in the analysis of nanoindentation. *J. Mater. Res.* **14,** 2296 (1999).
14. J. Alkorta, J.M. Martínez–Esnaola, and J. Gil Sevillano: Comments on "Comment on the determination of mechanical properties from the energy dissipated during indentation" by J. Malzbender [*J. Mater. Res.* **20**, 1090 (2005)]. *J. Mater. Res.* **21,** 302 (2006).
15. Y. Choi, H.S. Lee, and D. Kwon: Analysis of sharp-tip-indentation load-displacement curve for contact area determination taking into account pile-up and sink-in effects. *J. Mater. Res.* **19,** 3307 (2004).
16. M. Sakai: Simultaneous estimate of elastic/plastic parameters in depth-sensing indentation tests. *Scr. Mater.* **51,** 391 (2004).

17. V. Marx and H. Balke: A critical investigation of the unloading behavior of sharp indentation. *Acta Mater.* **45,** 3791 (1997).
18. J. Malzbender and G. de With: Indentation load–displacement curve, plastic deformation and energy. *J. Mater. Res.* **17,** 502 (2002).
19. J. Chen and S.J. Bull: A critical examination of the relationship between plastic deformation zone size and Young's modulus to hardness ratio in indentation testing. *J. Mater. Res.* **21,** 2617 (2006).
20. M. Li, W. Chen, N. Liang, and L. Wang: A numerical study of indentation using indenters of different geometry. *J. Mater. Res.* **19,** 73 (2004).
21. S. Soare: Design of a rotating sensor for stress measurement in metallization. Ph.D. Thesis, University of Newcastle upon Tyne, UK, 2004.
22. S. Jayaraman, G.T. Hahn, W.C. Oliver, C.A. Rubin, and P.C. Bastias: Determination of monotonic stress-strain curve of hard materials from ultra-low-load indentation tests. *Int. J. Solids Struct.* **35,** 365 (1998).
23. T.A. Venkatesh, K.J. Van Vleit, A.E. Ginnakopoulos, and S. Suresh: Determination of elasto-plastic properties by instrumented sharp indentation: Guidelines for property extraction. *Scr. Mater.* **42,** 833 (2000).
24. J.F. Palacio: Mechanical properties of high performance fullerene-like CN_x coatings assessed by nanoindentation. Ph.D. Thesis, University of Newcastle upon Tyne, UK, 2006.
25. Y.T. Cheng and C.M. Cheng: Further analysis of indentation loading curves: Effects of tip rounding on mechanical property measurements. *J. Mater. Res.* **13,** 1059 (1998).
26. J. Chen and S.J. Bull: On the relationship between plastic zone radius and maximum depth during nanoindentation. *Surf. Coat. Technol.* **201,** 4289 (2006).
27. H. Bei, E.P. George, J.L. Hay, and G.M. Pharr: Influence of indenter tip geometry on elastic deformation during nanoindentation. *Phys. Rev. Lett.* **95**(045501), 1 (2005).
28. J. Chen and S.J. Bull: Multicycling nanoindentation study on thin optical coatings on glass. *J. Phys. D: Appl. Phys.* **41,** 074009 (2008).